Principles of Hydroxamate Inhibition of Metalloproteases: Carboxypeptidase A†

William L. Mock* and Heng Cheng

Department of Chemistry, University of Illinois at Chicago, Chicago, Illinois 60607-7061

Received June 29, 2000; Revised Manuscript Received August 21, 2000

ABSTRACT: Hydroxamic acids of structure $RCON(OH)CH_2CH(CH_2C_6H_5)CO_2H$ induce micromolar competitive inhibition of catalysis for the enzyme carboxypeptidase A. Enzyme affinity depends on the nature of the acyl group, for RCO equaling HCO, CH_3CO, FCH_2CO, F_2CHCO, F_3CCO, CH_3OCH_2CO, or CH_3OCO. In acid dissociation these residues yield hydroxamic acid pK_a values that vary from 7.6 to 10.3. Profiles of inhibitory pK_i plotted versus pH indicate characteristically a maximum effectiveness near neutrality. Weaker binding to enzyme is generally displayed in either acidic or alkaline solution, with the position of the alkaline limb of the profiles depending on the pK_a of the inhibitor. A reverse-protonation pattern of association with the enzyme is indicated, in which the hydroxamate anion of the inhibitor displaces a relatively acidic H_2O ligand (pK_a of 6) from the active-site zinc ion of carboxypeptidase A. The metal-coordinating, N-substituted hydroxamic acid functional groups exist in solution as a mixture of syn and anti rotamers, with relative abundances that depend on their pK_a. A pyrrolidinone analogue having a conformationally syn-fixed cyclohydroxamic acid was not an especially potent inhibitor. Structure−activity relationships suggest design criteria for hydroxamic acid inhibitors in order to provide most effective binding with metalloenzymes.

Substrate analogues possessing hydroxamic acid functional groups have frequently been employed as inhibitors for zinc proteases, as well as for other metalloenzymes, because the favorable ligating ability of the RCONHOH moiety yields high enzyme affinity when the latter group interacts with an active site containing a transition metal ion. Such inhibitors are finding important application, for example, with matrix metalloproteinases, for which diverse peptide surrogates can be rendered effective inhibitors by incorporation of a hydroxamic acid residue (*1*−*7*). However, this type of inhibition has never been subjected to systematic scrutiny with regard to the hydroxamate functionality, such as would provide a basis for improved inhibitor design. We have undertaken to do so, employing carboxypeptidase A as the test enzyme, and with substrate analogue hydroxamic acid derivatives having constitution **1** (*8, 9*). The phenyl and carboxyl(ate) moieties within the structure of **1** are recognition elements providing enzymic specificity, much as occurs for catalytic substrates for carboxypeptidase, as well as for mimetic inhibitors such as the high-affinity ligand benzylsuccinic acid (*10*). By virtue of close analogy with the latter inhibitor, the RCONR′OH functionality present in **1** should adopt a position within an E·I complex allowing coordination with the active-site zinc ion (*11*). This is indicated to be the case by strong retardation of catalysis for carboxypeptidase A in the presence of **1**. Chemical variation within the nature of the R substituent (**a**−**g**) then provides structure and activity correlations that will be shown to characterize the inhibitor interaction with the enzyme. Inhibition by related pyrrolidinone **2** will also be considered.

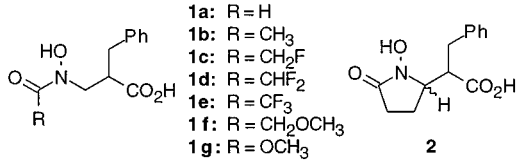

MATERIALS AND METHODS

Synthesis of Inhibitors. Preparations of **1a** and **1b** have been previously described, and it has been shown that only the L-enantiomer inhibits carboxypeptidase A (*8*). We have devised alternative preparations for **1** and **2**, which are furnished together with chemical characterizations, in the form of Supporting Information.

Enzyme and Buffers. Bovine pancreatic carboxypeptidase A (EC 3.4.17.1) was obtained from Sigma Chemical Co. (no. C 0386). It was recrystallized by dialysis according to established procedures before use (*12*). Enzyme concentrations were estimated using $\epsilon_{278} = 6.42 \times 10^4\ M^{-1}\ cm^{-1}$. Buffers employed in this work for kinetic analysis were (0.05 M each) as follows: 2-(*N*-morpholino)ethanesulfonic acid, pH of 5.5−7.0; tris-*N*-(hydroxymethyl)aminomethane, pH of 7.5−8.5; 2-amino-2-methyl-1,3-propanediol, pH of 9.0−10.0. All enzyme work was done with solutions 1.0 M in sodium chloride.

Kinetic Analysis. Kinetic assays for inhibition routinely employed the convenient substrate anisylazoformyl-L-phenylalanine (*13*), reported k_{cat}/K_m $4.1 \times 10^5\ M^{-1}\ s^{-1}$ at pH 7.7, or commonly at high pH, with the more traditional substrate *N*-[3-(2-furyl)]acryloyl-L-phenylalanyl-L-phenyla-

† This work was supported by the National Institutes of Health (GM39740).

* Address correspondence to this author: phone (312) 996-4897; e-mail wlmock@uic.edu; fax (312) 996 0431.

10.1021/bi001497s CCC: $19.00
Published on Web 10/21/2000

Table 1: Parameters Regulating Binding of Hydroxamic Acid Inhibitors **1** and **2** to Carboxypeptidase A in Saline Solution[a]

inhibitor (RC═O)	pK_{IH}[b]	pK_{EIH}[c]	K_i(lim) (μM)[d]	pK_d[e]	fraction syn[f]
1a (HCO)	8.38 ± 0.02	<5	1.39 ± 0.11[g]	8.24	0.66
1b (CH_3CO)	9.38 ± 0.01	5.4 ± 0.1	8.06 ± 0.41[h]	8.47	0.083
1c (FCH_2CO)	8.60 ± 0.02	<5	12.12 ± 0.68	7.52	0.007
1d (F_2CHCO)	7.95 ± 0.04	<5	2.59 ± 0.12	7.54	<0.001
1e (F_3CCO)	7.61 ± 0.02	<5	9.42 ± 1.06[i]	6.64	<0.001
1f (CH_3OCH_2CO)	9.01 ± 0.02	<5	9.07 ± 0.37	8.05	0.032
1g (CH_3OCO)	10.31 ± 0.04	5.8 ± 0.1	99.4 ± 3.4	8.31	~0.5[j]
2 ($-CH_2CH_2CO$)[k]	8.57 ± 0.02	<5	5.29 ± 0.61	7.84	1.0

[a] Inhibition constants have been obtained by logarithmic fit of data in Figures 1−3 to the equation in Scheme 1. [b] Spectrophotometrically determined value of pK_a for hydroxamic acid in saline solution. [c] Same ionization in EI complex, pK_a obtained from curve fitting (Figure 2). [d] Limiting value for K_i at intermediate pH. [e] Logarithmic constant, calculated for reverse-protonation mode of dissociation: $pK_d = pK_i(lim) + pK_{IH} - pK_{E1}$ (see Scheme 1). [f] Proportion of hydroxamic acid functional group present in syn rotameric conformation in protic medium (methanol). [g] Lit. K_i of 0.98 μM at unspecified pH (*8*). [h] Lit. K_i of 5.9 μM at unspecified pH (*8*). [i] An acidic-limb pK_a of 6.95 was obtained in the curve fit for this case, plus a threshold K_i of 0.4 mM (for competing pH-independent mode of binding). [j] At −30 °C a 1:1 ratio of rotamers was detected in $CDCl_3$ containing 20% CD_3OD. [k] Mixed diastereomers.

lanine [as employed for inset to Figure 1, wherein k_{cat}/K_m (lim) (9.0 ± 0.2) × 10^6 M^{-1} s^{-1}; pK_{E1} 5.98 ± 0.04; pK_{E2} 9.25 ± 0.04]. Velocity measurements for catalytic hydrolysis of the substrates were carried out at 25.0 (± 0.1) °C in buffers previously listed, with spectrophotometric analysis (anisylazoformyl, 350 nm, 2 cm path length) and the method of initial rates. Stock solutions of the anisylazoformylamide substrate should be shielded from light to avoid cis-trans isomerization of the azo linkage. Concentration of enzyme in assays was maintained well below substrate concentration for kinetic parameter determinations in all cases, and substrate concentration was well below K_m for competitive K_i measurements. Values for K_i at various pH were obtained by a direct fit of relative velocity measurements in the presence of varying amounts of hydroxamic acids to the equation for competitive inhibition. The limiting kinetic parameters were obtained by another nonlinear least-squares fit of K_i data to an appropriate equation, as given in Scheme 1. Our K_i values are for racemic substances **1** and **2**; correction for selective binding by only the L-enantiomer (*8*) would halve the values given. Acid dissociation constants for the inhibitors (pK_a values) were obtained by spectrophotometric titration in buffered 1 N sodium chloride solution, by monitoring a systematic increase in absorption near 230−250 nm at high pH (due to hydroxamate anion) and fitting the resulting curve (absorption versus pH) to a sigmoidal expression. All pH values in this article are calibrated pH meter readings uncorrected for ionic strength effects. Tolerances listed are standard errors from least-squares analysis.

RESULTS

By altering the nature of the R substituent in **1**, the acid dissociation of the hydroxamic acid residue, which interacts with the active-site Zn^{2+} ion in the carboxypeptidase−inhibitor complex, can be varied from a pK_a of 7.6 (**1e**, R = CF_3) to a pK_a of 10.3 (**1g**, R = OCH_3), as listed in Table 1 (column headed by pK_{IH}). The acid dissociation constants presented in the table in the form of pK_a values were obtained by spectrophotometric titration in the same buffered saline medium as used for enzyme kinetics. For these hydroxamates of varying acidity, competitive inhibition is engendered by incorporation of **1** in solution during kinetic assay of carboxypeptidase A (*8*). The K_i values for that inhibition exhibit a substantial range as a consequence of pK_a variation in **1a**−**g**, with the more acidic species generally yielding greater potency. Interpretation requires knowledge of pH dependence of K_i, which differs for each, as summarized in Figures 1 and 2 in the form of log−log plots (pK_i versus pH). For the most part these curves exhibit a maximum at intermediate pH, affording there a region of tightest binding to the enzyme ($pK_i = -\log K_i$). As will be outlined, that pattern arises as a consequence of "reverse-protonation" inhibition, which is common with metalloprotease inhibitors providing an especially effective ligand to the active-site metal ion (*14*−*22*). However, the family of pH profiles for **1** exhibits subtle variations, requiring additional explanation as provided subsequently. The most conspicuous feature of the data collectively is that the pH range established for most effective inhibition is broader for the less-acidic hydroxamic residues; i.e., the relative location of the alkaline limb of the profiles correlates with pK_a of the hydroxamic acid functional group, as is especially evident in Figure 2. That behavior is quite reasonable, since the ionizable functionality would become intimately involved in any E·I interaction.

Identification of a reverse-protonation mode of inhibition follows inescapably from the profiles, in conjunction with the chemical knowledge that metal chelation by hydroxamic acids commonly entails deprotonation of the ligand (eq 1) (*23*−*27*). Although a hydroxamate anion is certainly a much superior metal ligator relative to its conjugate acid counterpart, in the case of the present data binding of the inhibitors falls off at pH values that exceed the pK_a of the hydroxamic acid residue featured within the inhibitors (Figures 1 and 2: a lower value of pK_i occurring on the wing of a profile corresponds to weaker binding). The explanation for this anomaly is that the enzyme must take up an H^+ cation in order for the hydroxamate anion to coordinate to the active-site metal ion. Specifically, the obligatory protonation of a relatively acidic active-site residue on the enzyme must take place concurrently with hydroxamate anion binding. It will be shown that this requirement rationalizes the pH profiles.

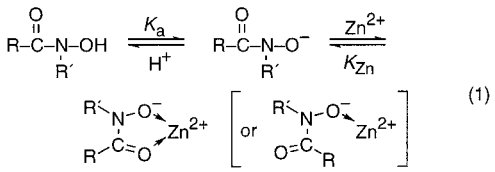

(1)

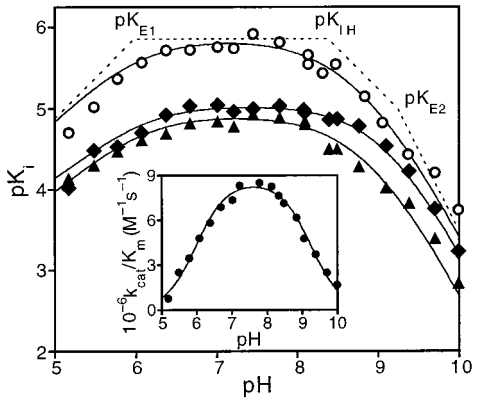

FIGURE 1: Dependence of pK_i ($-$log K_i) upon pH for **1a** (circles), **1f** (diamonds), and **1c** (triangles) for inhibition of carboxypeptidase A in buffered saline solution. Curves represent a least-squares (logarithmic) fit for an equation provided in Scheme 1, yielding parameters in Table 1. The asymptotic dashed line given for **1a** (slopes +1, 0, $-$1, and $-$2) contains breaks corresponding to pK_a values of groups present on enzyme or on inhibitor that regulate binding. Inset: pH dependence of catalysis by carboxypeptidase A (apparent value of k_{cat}/K_m for substrate *N*-[3-(2-furyl)]acryloyl-L-phenylalanyl-L-phenylalanine).

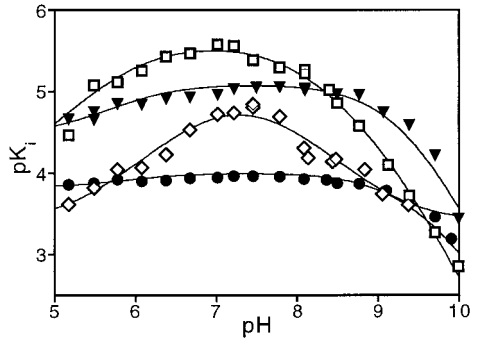

FIGURE 2: Dependence of pK_i ($-$log K_i) upon pH for **1d** (squares), **1b** (inverted triangles), **1e** (diamonds), and **1g** (filled circles) for inhibition of carboxypeptidase A in buffered saline solution. Curves are fitted as in Figure 1 (parameters in Table 1).

A plot of the velocity of substrate cleavage by carboxypeptidase A as a function of pH points to the enzymic proton acceptor. The kinetic parameter k_{cat}/K_m, a second-order rate constant for catalysis under conditions of low substrate concentration, shows a characteristic bell shape in its acid dependence (inset to Figure 1). As has previously been shown on numerous occasions (*15, 28*−*30*), this reveals the presence of two enzymic functional groups governing catalysis, having true pK_a values (*31*) measured here as 6.0 and 9.25 (pK_{E1} and pK_{E2}, respectively). One group must necessarily be protonated and the other obligatorily deprotonated in order for substrate binding and conversion to take place. Inspection of the profiles in Figures 1 and 2 suggests that these same enzymic functional groups are influencing binding of hydroxamate inhibitor as well. In particular, the pK_{E1} group of 6.0 must be required to adopt its protonated form in order for the inhibitor anion to link tightly with the active-site metal ion. Should that be the case, the existence of a maximum in the value of pK_i at intermediate pH is explained. At pH values greater than 6, the fraction of enzyme susceptible to inhibition diminishes, due to ionization of that residue. However, a compensatory change occurs in the inhibitor. At pH values lower than the hydroxamic acid pK_a (values of which range from 7.6 to 10.3), the available fraction of coordinating anion in solution progressively decreases, due to protonation. In consequence, these factors cancel one another, and the inhibition profile emerges as level at intermediate pH values. Enzyme−inhibitor affinity decreases on the acidic limb of the profile because even less hydroxamate anion is available, although the enzyme becomes fully susceptible to inhibition there because the pK_{E1} residue protonates entirely in acid. Likewise, binding also falls off on the alkaline limb, where the inhibitor becomes fully ionized and best capable of ligation, but the enzyme becomes even more severely depleted as regards protonation of the critical enzymic residue of pK_a 6. This pattern is known as reverse protonation inhibition, because it appears that a metastable protonation state within the E·I complex is involved in formation of the tightly bound adduct.

An identity of the critical enzymic pK_{E1} residue is not provided by the kinetic evidence but can be supplied by chemical reasoning. In the absence of substrate or inhibitor, a solvent water molecule ligates to the active-site Zn^{2+} of carboxypeptidase A (*32*). Because that zinc ion has been rendered hyper(Lewis)acidic for purposes of catalytic efficacy, the enzymic Zn^{2+}·OH_2 moiety attains a protonic pK_a of 6 in consequence (*19*). This yields the only plausible explanation for the gross shape of the pK_i versus pH profiles. A hydroxamate anion can displace H_2O from the zinc ion, but it cannot displace hydroxide (HO^-), so that control of inhibitor binding by this Zn^{2+}·OH_2 residue is absolute. Formerly, it has been believed (with ambiguous supporting evidence) that the side-chain carboxyl of enzymic residue Glu 270 was responsible for pK_{E1}. This is a catalytically essential residue, with a counterpart present in the active site of most other metalloproteases. However, that explanation is untenable. If it were Glu 270 that regulates ligation of hydroxamate, that residue would have to possess a pK_a of $>$10 within the E·I complex, since the falloff for pK_i in alkaline solution is provided mainly by the necessity of the pK_{E1} functional group to be protonated at that pH in order for binding to occur. Not only is that mechanistically unreasonable for a carboxylic acid, but a similar requirement for protonation when chemically comparable substrates are bound would logically mean that the carboxylate ion Glu 270-$CH_2CH_2CO_2^-$ could not be present for catalytic purposes within E·S. Either the metal-bound water molecule being displaced is the acidic enzyme residue observed kinetically, or catalysis mechanisms that rely upon an anionic glutamate side chain cannot be valid, unless Glu 270-$CH_2CH_2CO_2^-$ were to yield an opposite effect on binding of substrates. That catalytically essential side-chain carboxyl group in all likelihood has a normal pK_a of ~4, a value that is too low to be detected in the enzyme kinetics or in the inhibition profiles.[1]

While reverse-protonation inhibition explains the overall shape of the pH dependence of pK_i for the hydroxamic acids with carboxypeptidase A, there are additional perturbations evident in the profiles that refine understanding of the E·I

[1] Because the Glu-$CH_2CH_2CO_2H$ and Zn^{2+}·OH_2 groups reside within H-bonding distance of one another in the enzyme, it cannot be excluded that their ionizations should mutually influence each other. However, the measured pK_a of 6 would be the *second* ionization of such a coupled system. For the related enzyme thermolysin, a reverse-protonation catalytic mechanism has been advanced (*33*) to rationalize the characteristic pH profile for k_{cat}/K_m (inset to Figure 1).

complexes. The least acidic of the hydroxamic acids, **1g** in Figure 2, also exhibits diminishing inhibition at pH values of >9, which occurs a full pH unit below the ionization of the hydroxamic group. Several other inhibitors of slightly greater acidity (**1c**−**1f**) show for K_i an inverse second-order dependence on acid concentration in this pH range, as is specifically designated for **1a** in Figure 1 by the descending asymptote with a slope of −2 on the extreme alkaline limb of the profile. Apparently the other enzymic residue detected kinetically in alkaline solution in the plot of k_{cat}/K_m versus pH (pK_{E2}, inset to Figure 1) also influences inhibitor binding. Its ionization occurring at high pH further causes the enzyme to reject hydroxamate inhibitor. The responsible enzymic functional group is not readily identified. It cannot be the metal-bound water molecule, for that ionization must be assigned to pK_{E1}, to explain the overall convex shape of the profiles as previously discerned. A possible assignment could be one of the imidazole rings found in the two histidine residues which participate in holding the catalytic zinc ion at the active site (His 72, His 196). Coordination by one of the nitrogens of an imidazole ring to a Lewis acid such as Zn^{2+} acidifies the proton on the other imidazole nitrogen of that ring (eq 2). As shown by model studies, a pK_a of 9−10 is chemically reasonable for such a deprotonation (occurring at a pH midway between the first and second acid dissociations of the parent imidazolium ion; *34*−*36*), and NMR investigations of cobalt-carboxypeptidase A support this assignment (*15*, *37*). The ligation of an enzymic imidazolate anion to the active-site Zn^{2+}, as yielded by such a deprotonation, would diminish the effective Lewis acidity of that metal ion, so that by reflex it would bind the hydroxamate moiety of the inhibitor more weakly. That could account for the extra release of inhibitor seen in the pH profiles in alkaline solution. However, the measurable perturbation of K_i attributable to pK_{E2} is small, when compared to the absolute control exerted by pK_{E1}, and some other enzymic ionization near the active site could easily be responsible instead.

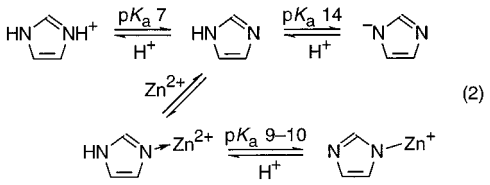

(2)

For inhibitors **1b** and **1g**, the acidic limb of the pH profiles in Figure 2 does not descend in the manner exhibited for the other hydroxamates. An explanation lies in the limited intrinsic acidity of these hydroxamic acids (pK_a values of ≥9.4). The leveling-off within pK_i at lower pH in these cases is to be attributed to protonation of the hydroxamate anion within the E·I complex, setting up an acid dissociation for which a pK_a value can be derived by curve-fitting (pK_{EIH}). Expressed equivalently, the hydroxamic acid form of the inhibitor also binds to the enzyme, albeit much more weakly than does the hydroxamate anion. However, the population of anionic form in solution ($RCONR'O^-$) for these nonacidic metal ligators is severely depleted at pH values below 6, so that enzymic inhibition by the more abundant conjugate acid form becomes comparable to that of the anion. The fact that other inhibitors of structure **1** do not show this leveling off in pK_i is merely a consequence of their greater intrinsic acidity. The equivalent inflection for them must take place at a pH of <5, measurement of which is impractical due to enzyme instability in acidic solution. In short, recognition that the variation in position of pK_{EIH} in the profiles correlates with hydroxamic acid acidity diagnoses that pK_a as a perturbed inhibitor ionization.

In this conjunction it should be acknowledged that catalysis is also blocked by the protoligand phenylpropionic acid ($C_6H_5CH_2CH_2CO_2H$), which embodies within itself the partial structure of **1** that yields enzymic specificity. This substance functions as an anionic inhibitor for carboxypeptidase A with a competitive K_i value of 0.02 mM at pH 6 (*38*). Hence, the leveling-off within pK_i seen especially for **1b** and **1g** on the acidic limb of the pH profiles in Figure 2 may have a trivial explanation. It may correspond merely to conversion from a coordinative mode of binding by the hydroxamate anion to an active-site occupancy by the protonated form of **1,** in which the latter need not involve ligation of inhibitor side chain to the metal ion at all, since that mode of binding ought to have a K_i value similar to that of phenylpropionic acid, as does indeed transpire for **1b** and **1g** at low pH. For the weak inhibitor **1e**, a leveling-off of its profile on both the acidic and alkaline limbs suggests an additional simultaneous and competitive mode of inhibition, lacking a pH dependence but with a K_i of ∼0.4 mM, as derived from the curve fit shown in Figure 2 for that species.

Scheme 1

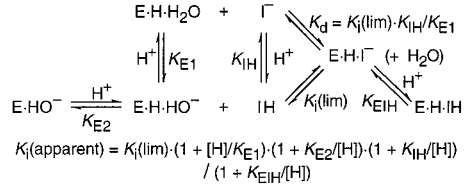

$$K_i(\text{apparent}) = K_i(\text{lim})\cdot(1 + [H]/K_{E1})\cdot(1 + K_{E2}/[H])\cdot(1 + K_{IH}/[H]) / (1 + K_{EIH}/[H])$$

The preceding comprehensive explanation of the inhibition profiles, applicable to all of the hydroxamates, is summarized in Scheme 1. In this composite formulation K_{E1} and K_{E2} represent the ionizations of the enzyme that have been independently and repeatedly shown to affect catalysis kinetics: a pK_{E1} of 6.0 for $E{\cdot}H{\cdot}H_2O \rightarrow E{\cdot}H{\cdot}HO^-$ and a pK_{E2} of 9.25 for $E{\cdot}H{\cdot}HO^- \rightarrow E{\cdot}HO^-$, both derived from the inset to Figure 1. These values have been inserted as nonadjustable parameters in the fitted inhibition curves of Figures 1 and 2 for **1a**−**g**. Likewise, K_{IH} represents the acid dissociation constant of the hydroxamic acid functional group of the inhibitors, an item that has been independently determined by spectrophotometric titration for each variant of structure **1** in saline solution in the absence of enzyme. For the functionality so designated in Scheme 1 as IH, pertinent pK_a values range from 7.6 to 10.3 depending on acyl substituent, and that acid dissociation K_{IH} is also included appropriately as a fixed parameter in each curve fit. The only adjustable parameters needed to accommodate the individual profiles for the full set inhibitors are then K_{EIH}, an ionization of the enzyme−inhibitor complex providing a minor perturbation on the acidic limb in a few cases as just described, plus a limiting value for the inhibition constant for each variant of **1** at intermediate pH, given by K_i(lim), the numerical values for which are listed in Table 1. However, the latter constants

correspond empirically to ligation between IH and E·H·OH^-, the uncombined forms of inhibitor and enzyme that actually predominate at intermediate pH (lower half of Scheme 1). Because H^+ location cannot be discerned kinetically, chemical combination of those two entities is indistinguishable in principle from association between the hydroxamate anion form of inhibitor (I^-) and the protonated form of enzyme (E·H·H_2O), which corresponds to the manner in which the pH profiles were rationalized previously (upper half of Scheme 1). For the latter reaction, which has an identical net stoichiometry, a dissociation constant (K_d) may also be defined as included in Scheme 1. It may be shown thermodynamically that this K_d necessarily equals numerically the value of K_i(lim) multiplied by the ratio of the acid dissociation constants for inhibitor and enzyme, which residues govern reverse protonation (K_{IH} and K_{E1}). Quantitative values for each of the pertinent constants are provided in Table 1, in the form of kinetic parameters as secured by curve fitting in the figures. The fact that the disparate curve shapes in Figures 1 and 2 can be uniquely reconciled for all inhibitors within a single scheme, employing only one major adjustable parameter, K_i(lim), lends credence to the interpretation.

Geometrically, inhibitors **1** exist in solution as a mixture of syn and anti conformational rotamers with respect to the RCO−N(R′)OH linkage (eq 3). The ratio depends on the nature of the acyl substituent, and that too should influence enzyme binding efficiency. Only the syn (*Z*) form may chelate a metal ion, but that rotamer appears to be disfavored in hydroxylic media, where external H-bonds to the anti (*E*) conformer may compete with an internal H-bond bridge occurring in the syn form (*39*, *40*). An effort was made to account for this factor by NMR spectroscopy. At low temperature the rotamers interconvert sufficiently slowly ($k \leq 80\ s^{-1}$) that a separate set of signals may be detected from each, and the population distribution may then be estimated for several of the inhibitors. The final column in Table 1 gives the fraction of syn rotamer present in methanolic solution. That has been directly ascertained for **1a** and **1b** in CD_3OD, and for **1c** and **1f** the abundance has been estimated by determination in $CDCl_3$ where the ratio is more suitable for measurement, with application of an empirical correction for H-bonding as secured from the syn−anti perturbation noted for **1b** upon transfer from $CDCl_3$ to CD_3-OD. The rotamer distribution in methanol approximates that in aqueous solution (as pertains for inhibition); in fact, as little as 5% methanol in chloroform provides sufficient intermolecular H-bonding to maximize the anti form. In general, the amount of potentially chelating syn rotamer appears to diminish in response to decreasing pK_a of the hydroxamic acid residue. This presumably reflects less favorable intramolecular H-bonding of the type depicted for the syn form in eq 3, when the carbonyl oxygen relinquishes basicity due to presence of an electron-withdrawing acyl substituent. For the more acidic species **1d** and **1e** the fraction of syn rotamer was too small to measure in any solvent. An exception is the methoxycarbonyl group in **1g**; it can intramolecularly H-bond while in either conformation about the CO−N linkage, and the presence of a 1:1 mixture of rotamers at −30 °C suggests that to be the case. However, a steric factor as regards the acyl moiety (repulsion between R and R′ in eq 3) must also influence the syn/anti ratio, because the formyl derivative **1a** (R = H) has a disproportionately large amount of syn rotamer for its pK_a value. Since **1a** binds to the enzyme especially well, this may be a significant determinant of inhibitor efficacy, as needs to be considered.

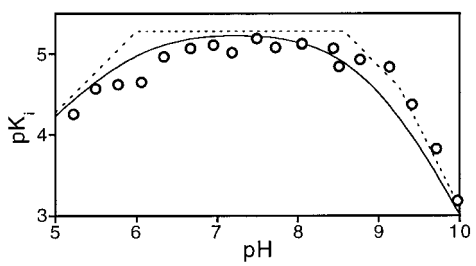

FIGURE 3: Dependence of pK_i (−log K_i) upon pH for inhibition of carboxypeptidase A by **2** in buffered saline solution. Curve is fitted as in Figure 1 (asymptotic dashed line contains breaks corresponding to pK_a values, parameters in Table 1).

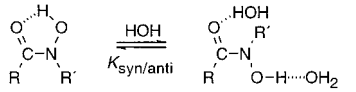

(3)

An attempt was made to control rotameric distribution favorably by examination of inhibitory properties of analogous structure **2**. Incorporation within a pyrrolidinone ring fixes the hydroxamic acid moiety in a syn conformation. Because of the introduction of an additional stereogenic center in the five-membered ring, this inhibitor could only be obtained as an inseparable mixture of diastereomers, present in similar amounts according to NMR. Structural modeling suggested that both should be able to ligate to the active site of carboxypeptidase A. The mixture of substances was submitted to the enzyme, with the reasoning that even if only one were actually to bind, the resulting gross K_i value could only be in error by a factor of 2, since the diastereomers were equally abundant. The results of a pH-dependence study of K_i for **2** are summarized in Figure 3, and behavior comparable to **1** is indicated, with observance of the expected influence of acid dissociations on binding. Overall inhibitor affinity for the enzyme is specified by the limiting K_i value, given in Table 1. The gross K_i of 5.3 μM does not differ markedly from that for members of series **1** having a similar acidity but possessing negligible syn content. Although steric factors, including choice of heterocyclic ring size, may account for a lack of superiority for **2**, it appears not to represent a promising strategy for enhancing enzymic affinity in the case of carboxypeptidase A.

DISCUSSION

The purpose of this investigation was to discern the factors contributing to most effective hydroxamate inhibition of carboxypeptidase A. The overall pattern that has emerged indicates that the reverse protonation mode of inhibitor binding prevails, such as has previously been demonstrated with a set of comparably acidic phenol-containing inhibitors (*14*, *15*, *19*). In complexation, the anion from the weakly acidic inhibitor ligand displaces a somewhat more acidic H_2O ligand (pK_a of 6) from the enzymic active-site Zn^{2+}, resulting in maximum affinity at intermediate pH. A high content of syn rotamer in solution, as may be resolved by NMR spectroscopy for the linkage RCO−N(R′)OH, might have been expected to furnish tightest binding, should a chelative

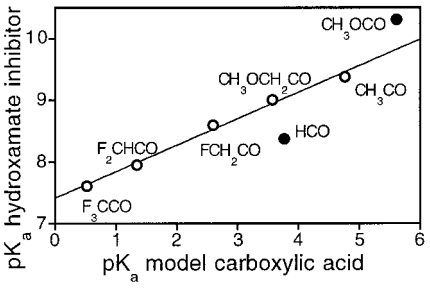

FIGURE 4: Plot of pK_a values for **1** (in 1 N NaCl) versus pK_a values for corresponding model carboxylic acids, RCO_2H, in nonsaline solution. Labels identify acyl residues (RC═O) for each. The least-squares regression line (for open circles) has a slope of 0.43 ± 0.02 and an intercept of 7.41 ± 0.07; only acetyl derivatives are included in the line fit. Carboxylic acid pK_a values are from ref *43*; methylcarbonic acid CH_3OCO_2H, pK_a 5.61 (*44*).

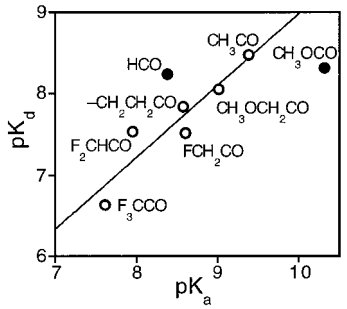

FIGURE 5: Plot of pK_d [= pK_i(lim) + pK_{IH} − pK_{E1}] for carboxypeptidase A plus **1** and **2** versus pK_a for the hydroxamic acid residue (pK_{IH}) in saline solution. The regression line has a slope of 0.88 ± 0.17 and an intercept 0.2 ± 1.5 (for open symbols only).

mode of hydroxamate-group ligation prevail in the E·I complexes. For unconstrained acetohydroxamic acids **1**, the potentially less inhibitory anti rotamer is generally favored in aqueous solution. But the cyclic hydroxamate moiety of **2**, with 100% syn content, binds only slightly better than **1c**, with <1% syn content, while the anions of both have a similar proton affinity. Although metal chelation involving **1** or **2** probably is feasible (*3, 4, 6, 21, 27*), bidentate Zn^{2+} coordination within the enzymic complexes may not actually be important, since only one labile aquo ligand is found attached to the active-site zinc ion for the native enzyme in the case of carboxypeptidase A. Ordinarily, the chelation effect in metal ligation is largely entropy-driven (*41*). The phenomenon arises normally from replacement of two or more solvent molecules within the coordination sphere of a metal ion by a single polydentate species, with an attendant net increase in translational and rotational degees of freedom overall. If only one solvent molecule is available for release, as with carboxypeptidase A, the effect should be diminished. The anti rotamer of the inhibitor anion may actually be the species prevalent in some E·**1** complexes (eq 1; nonchelative binding of a single hydroxamate oxyanion moiety to Zn^{2+}).

The relationship between hydroxamic acid pK_a and potency of enzymic inhibition merits special attention. The chemical nature of the acyl group within a hydroxamic acid systematically influences its acidity. The perturbation of pK_a from that source is summarized most succinctly in Figure 4. A plot of pK_a for the hydroxamic acids **1b**−**f** versus the pK_a of the correspondingly substituted acetic acid (RCO_2H, open circles) yields a least-squares linear slope of 0.43 ± 0.02. This correlation indicates that ionization of an N-substituted hydroxamic acid is 0.43 times as sensitive to electron withdrawal in comparison to a carboxylic acid, which follows from the labile proton being situated one additional atom removed from the acyl moiety within the hydroxamic acids. In each of the compared structural types, the degree of acidification arises from a combination of inductive and conjugative contributions from the acyl moiety. That, plus solvation differences and a possible syn−anti conformational effect, accounts for the displacement from the regression line of the points for the formyl and methoxycarbonyl groups (**1a**, **1g**; filled circles), which entail a different mix of these factors for the two kinds of acids being plotted against one another. For that reason the linear correlation that is shown only incorporates the acetyl derivatives (open circles). However, the coefficients derived from the plot should enable a practical estimate of the pK_a of any N-alkylated hydroxamic acid when that for the corresponding carboxylic acid is available.

The next step as regards interpretation of enzymic ligation by **1** is to account for the influence of hydroxamic acid pK_a on the affinity of inhibitors for carboxypeptidase A. Generally, one should expect that greater proton attraction on the part of the hydroxamate anion should also yield higher enzyme affinity, due to a stronger potential linkage to the active-site zinc ion, and because each process subsumes such a (Lewis)acid−base interaction. This entails a ligand comparison of pK_a values with pK_d values, since the latter directly expresses the association of inhibitor anion with the receptive form of enzyme (Scheme 1; K_d against K_{IH} represents a competition for I^-). Such an equating of logarithmic constants yields a free energy correlation, and a linear response might be anticipated, similar to that attained in Figure 4. The corresponding plot is provided in Figure 5, and indeed there appears to be a positive connection between proton affinity and enzymic binding for the various hydroxamate inhibitors (slope ≈ 0.9) but with considerable scatter in the data. In the computation of slope, **1a** and **1g** have been excluded, since they display a misalignment comparable to that in Figure 4, perhaps for similar reasons. In particular, the formyl derivative **1a** exhibits a significant positive deviation from the regression line; i.e., it seems to bind better than expected on the basis of its pK_a value. Although **1a** in solution has an especially high concentration of syn rotamer about the RCO−N(R′)OH linkage, that would appear not to be the explanation for tighter binding, based on the unexceptional affinity of **2** for the enzyme as previously considered. In size the formyl residue of **1a** is the smallest of the set, so an additional unfavorable steric interaction with the enzyme could be adversely affecting the other inhibitors.

With reservations regarding ambiguity from the scatter of data points, the slope of the regression line in Figure 5 contains useful information. It represents an appropriately corrected comparison involving the affinity of the active-site Zn^{2+} for the inhibitor oxyanion, versus the affinity of solvent proton H^+ for the same species. A coefficient of 0.9 means that the active-site zinc ion has a Lewis acidity character very nearly equivalent to that of a proton, as measured by coordination to a common type of Lewis base (the hydroxamate oxyanion). Elsewhere, we have shown how such hyper(Lewis)acidity of that metal ion helps to explain catalytic efficacy (as well as the magnitude of K_{E1} for the enzyme, an ionization attributed to Zn^{2+}·OH_2; *19*). As a

practical matter, the amplitude of this empirical slope coefficient means that some advantage can be gained from employing more acidic hydroxamic acids within inhibitors, as in the following analysis.

By way of conclusion, the design criteria for improvement of hydroxamate inhibitors suggested by this study are as follows. The pK_a of the hydroxamic acid moiety should be adjusted, for example, by attachment of electron-withdrawing substituents, so as to approximate the pH of the medium in which the inhibitor is to operate. This specification is a consequence of the reverse-protonation mechanism of inhibition, in which the conjugate acid form of enzyme in effect competes with hydronium ions for coordination to the hydroxamate anion. Facilitation of anion formation by a lower inhibitor pK_a promotes reverse-protonation binding, at the expense of some diminution of the strength of the resulting hydroxamate-to-Zn^{2+} interaction. However, so long as the slope of the regression line in Figure 5 is less than unity, the gain in anion population in solution associated with decrease of pK_a outweighs curtailed zinc−hydroxamate affinity, and so in principle an increase in the acidity of the hydroxamic acid yields a net benefit as regards practical tightness of binding. But this advantage disappears should the inhibitor pK_a value fall below the intended pH of operation, since the proportion of free anion then enters a plateau, while the weakened zinc binding from a less-basic hydroxamate ligand further diminishes pK_i. Hence, the inhibitor pK_a should nearly match the pH of the target enzyme's native environment. In some cases adoption of a syn conformation for the hydroxamate might beneficially be reinforced, for instance, by incorporation into a heterocyclic structure such as **2**. However, that is likely to help only for active-site metal ions that are susceptible to buttressing by chelative coordination; i.e., when the catalytic mechanism is such that more than one ligand can be displaced by the bidentate inhibitor. By following this reasoning, an optimal hydroxamate for inclusion in a contemplated metalloenzyme inhibitor may be rationally selected.

There are implications from this study for understanding of the catalytic mechanism of the metalloproteases. To design a metal-ligating inhibitor according to the logic in the previous analysis, it is necessary to appreciate the enhanced acidity of the water molecule bound to the active-site metal ion in the absence of inhibitor or substrate. Specifically, the enzymic pK_{E1} value of 6 arising from deprotonation of Enz-Zn^{2+}·OH_2 absolutely controls the reverse-protonation mode of inhibitor binding to carboxypeptidase A, and that must be acknowledged in devising an inert and tenacious active-site occupant for the enzyme. As a consequence of this pK_a, hydroxide is the prevalent metal ligand present in the uncomplexed enzyme at pH values yielding maximum catalytic activity (Figure 1, inset). The characteristic pH profiles for hydroxamic acid inhibition arise only because OH^- cannot be displaced from zinc by hydroxamate anion, without protonation. This practical matter of Enz-Zn^{2+}·OH_2 hyperacidity, a perception sufficiently important as to be essential for rational inhibitor design, ought to figure prominently in any formulation of a catalytic mechanism for metalloproteases. Yet, the most widely cited peptide cleavage scheme for operation of these enzymes does not fit this realization. That particular mechanism (*42*) is premised on a higher pK_a for the metal-bound water molecule and contains a speculation that a critical enzymic general base (a side-chain glutamic carboxylate) is necessary to accomplish deprotonation of Enz- Zn^{2+}·OH_2 during catalysis, a proton transfer that actually should not be necessary since the enzyme already exists largely in deprotonated form at this site. Fortunately, an alternative interpretation of catalysis is available, employing a reverse-protonation chemical mechanism that is capable of explaining why such enzymes work, as well as how (*22*, *33*).

SUPPORTING INFORMATION AVAILABLE

Preparations and chemical characterization of substances **1a**−**g** and **2** and NMR spectra illustrating temperature and solvent-composition dependence of syn−anti geometry for **1a** and **1b**. This material is available free of charge via the Internet at http://pubs.acs.org.

REFERENCES

1. Levy, D. E., Lapierre, F., Liang, W. S., Ye, W. Q., Lange, C. W., Li, X. Y., Grobelny, D., Casabonne, M., Tyrrell, D., Holme, K., Nadzan, A., and Galardy, R. E. (1998) *J. Med. Chem. 41*, 199−223.
2. Yamamoto, M., Tsujishita, H., Hori, N., Ohishi, Y., Inoue, S., Ikeda, S., and Okada, Y. (1998) *J. Med. Chem. 41*, 1209−1217.
3. Xue, C. B., He, X. H., Roderick, J., Degrado, W. F., Cherney, R. J., Hardman, K. D., Nelson, D. J., Copeland, R. A., Jaffee, B. D., and Decicco, C. P. (1998) *J. Med. Chem. 41*, 1745−1748.
4. Jacobson, I. C., Reddy, P. G., Wasserman, Z. R., Hardman, K. D., Covington, M. B., Arner, E. C., Copeland, R. A., Decicco, C. P., and Magolda, R. L. (1998) *Bioorg. Med. Chem. Lett. 8*, 837−842.
5. Marcotte, P. A., Elmore, I. N., Guan, Z. W., Magoc, T. J., Albert, D. H., Morgan, D. W., Curtin, M. L., Garland, R. B., Guo, Y., Heyman, H. R., Holms, J. H., Sheppard, G. S., Steinman, D. H., Wada, C. K., and Davidsen, S. K. (1999) *J. Enzyme Inhib. 14*, 425−435.
6. Cherney, R. J., Wang, L., Meyer, D. T., Xue, C. B., Arner, E. C., Copeland, R. A., Covington, M. B., Hardman, K. D., Wasserman, Z. R., Jaffee, B. D., and Decicco, C. P. (1999) *Bioorg. Med. Chem. Lett. 9*, 1279−1284.
7. Duan, J. J. W., Chen, L. H., Xue, C. B., Wasserman, Z. R., Hardman, K. D., Covington, M. B., Copeland, R. R., Arner, E. C., and Decicco, C. P. (1999) *Bioorg. Med. Chem. Lett. 9*, 1453−1458.
8. Kim, D. H., and Jin, Y. (1999) *Bioorg. Med. Chem. Lett. 9*, 691−696.
9. Jin, Y., and Kim, D. H. (1998) *Bioorg. Med. Chem. Lett. 8*, 3515−3518.
10. Byers, L. D., and Wolfenden, R. (1973) *Biochemistry 12*, 2070−2078.
11. Mangani, S., Carloni, P., and Orioli, P. (1992) *J. Mol. Biol. 223*, 573−578.
12. Mock, W. L., and Chen, J.-T. (1980) *Arch. Biochem. Biophys. 203*, 542−552.
13. Mock, W. L., Liu, Y., and Stanford, D. J. (1996) *Anal. Biochem. 239*, 218−222.
14. Mock, W. L., and Tsay, J.-T. (1986) *Biochemistry 25*, 2920−2927.
15. Mock, W. L., and Tsay, J.-T. (1988) *J. Biol. Chem. 263*, 8635−8641.
16. Mock, W. L., and Aksamawati, M. (1994) *Biochem. J. 302*, 57−68.
17. Mock, W. L., and Tsay, J.-T. (1989) *J. Am. Chem. Soc. 111*, 4467−4472.
18. Mock, W. L., and Zhang, J. Z. (1991) *J. Biol. Chem. 266*, 6393−6400.
19. Mock, W. L., Freeman, D. J., and Aksamawati, M. (1993) *Biochem. J. 289*, 185−193.

20. Mock, W. L., and Green, P. C. (1990) *J. Biol. Chem. 265*, 19606−19610.
21. Mock, W. L., and Yao, J. (1997) *Biochemistry 36*, 4949−4958.
22. Mock, W. L. (1998) in *Comprehensive Biological Catalysis* (Sinnott, M., Ed.) Vol. 1, Chapt. 11, pp 425−453, Academic Press, London.
23. Schwarzenbach, G., and Schwarzenbach, K. (1963) *Helv. Chim. Acta 46*, 1390−1400.
24. Monzyk, B., and Crumbliss, A. L. (1979) *J. Am. Chem. Soc. 101*, 6203−6213.
25. Parekh, P. C., Manon, S. K., and Agrawal, Y. K. (1989) *J. Chem. Soc., Perkin Trans. 2*, 1117−1123.
26. Zalkin, A., Forrester, J. D., and Templeton, D. H. (1966) *J. Am. Chem. Soc. 88*, 1810−1814.
27. Holmes, M. A., and Matthews, B. W. (1981) *Biochemistry 20*, 6912−6920.
28. Hall, P. L., Kaiser, B. L., and Kaiser, E. T. (1969) *J. Am. Chem. Soc. 91*, 485−491.
29. Auld, D. S., and Vallee, B. L. (1970) *Biochemistry 9*, 4352−4359.
30. King, S. W., and Fife, T. H. (1983) *Biochemistry 22*, 3603−3610.
31. Cleland, W. W. (1990) in *The Enzymes*, Vol. XIX, pp 99−158, Academic Press, New York.
32. Rees, D. C., Lewis, M., and Lipscomb, W. N. (1983) *J. Mol. Biol. 168*, 367−387.
33. Mock, W. L., and Stanford, D. J. (1996) *Biochemistry 35*, 7369−7377.
34. Bauman, J. E., and Wang, J. C. (1964) *Inorg. Chem. 3*, 368−373.
35. Forsling, W. (1977) *Acta Chem. Scand. A31*, 759−766.
36. Sundberg, R. J., and Martin, R. B. (1974) *Chem. Rev. 74*, 471−517.
37. Bertini, I., Gerber, M., Lanini, G., Luchinat, C., Maret, W., Rawer, S., and Zeppezauer, M. (1984) *J. Am. Chem. Soc. 106*, 1826−1830.
38. Fukuda, M., Kunugi, S., and Ise, N. (1983) *Bull. Chem. Soc. Jpn. 56*, 3308−3313.
39. Walter, W., and Schaumann, E. (1971) *Liebigs Ann. Chem. 743*, 154−166.
40. Brown, D. A., Glass, W. K., Mageswaran, R., and Mohammed, S. A. (1991) *Magn. Reson. Chem. 29*, 40−45.
41. Fersht, A. (1999) in *Structure and Mechanism in Protein Science*, Chapt. 11, p 345, W. H. Freeman, New York.
42. Matthews, B. W. (1988) *Acc. Chem. Res. 21*, 333−340.
43. Serjeant, E. P., and Dempsey, B. (1979*) Ionization Constants of Organic Acids in Aqueous Solution*, Pergamon Press, Oxford, U.K.
44. Gattow, G., and Behrendt, W. (1972) *Angew. Chem., Int. Ed. Engl. 11*, 534−535.

BI001497S